From Formamide to Purine: A Self-Catalyzed Reaction Pathway Provides a Feasible Mechanism for the Entire Process

ARTICLE *in* THE JOURNAL OF PHYSICAL CHEMISTRY B · AUGUST 2013

Impact Factor: 3.3 · DOI: 10.1021/jp404540x · Source: PubMed

THE JOURNAL OF PHYSICAL CHEMISTRY B

Article

pubs.acs.org/JPCB

From Formamide to Purine: A Self-Catalyzed Reaction Pathway Provides a Feasible Mechanism for the Entire Process

Jing Wang,[†] Jiande Gu,*[,†,‡] Minh Tho Nguyen,[§] Greg Springsteen,[∥] and Jerzy Leszczynski*[,†]

[†]Interdisciplinary Nanotoxicity Center, Department of Chemistry, Jackson State University, Jackson, Mississippi 39217, United States

[‡]Drug Design and Discovery Center, State Key Laboratory of Drug Research, Shanghai Institute of Materia Medica, CAS, Shanghai 201203, People's Republic of China

[§]Department of Chemistry, University of Leuven, B-3001 Leuven, Belgium

[∥]Department of Chemistry, Furman University, 3300 Poinsett Highway, Greenville, South Carolina 29613, United States

Supporting Information

ABSTRACT: A formamide self-catalyzed mechanistic pathway that transforms formamide to purine through a five-membered ring intermediate has been explored by density functional theory calculations. The highlight of the mechanistic route detailed here is that the proposed pathway represents the simplest and lowest energy reaction pathway. All necessary reactants, including catalysts, are generated from a single initial compound, formamide. The most catalytically effective form of formamide is found to be the imidic acid isomer. The catalytic effect of formamide has been found to be much more significant than that of water. The self-catalytic mechanism revealed here provides a pathway with the lowest energy barriers among all reaction routes previously published. Several important reaction steps are involved in this mechanistic route: formylation−dehydration, Leuckart reduction, five- and six-member ring-closing, and deamination. Overall, a five-membered ring-closing is the rate-determining step in the present catalytic route, which is consistent with our previous mechanistic investigations. The activation energy of this rate-controlling step (ca. 27 kcal/mol) is significantly lower than the rate-determining step (ca. 34 kcal/mol) in the pathway from 4-aminoimidazole-5-carboxamidine described by Schleyer's group (*Proc. Natl. Acad. Sci. U.S.A.* **2007**, *104*, 17272−17277) and in the pyrimidine pathway (ca. 44 kcal/mol) reported by Sponer et al. (*J. Phys. Chem. A* **2012**, *116*, 720−726). The self-catalyzed mechanistic pathway reported herein is less energetically demanding than previously proposed routes.

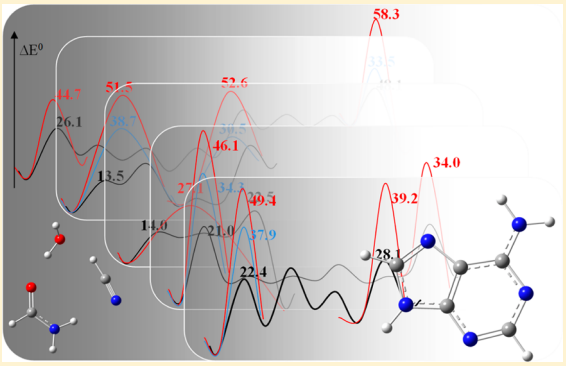

INTRODUCTION

The origin of primitive biomolecules leading to a proto-metabolism is one of the most significant unsolved puzzles in science.[1−3] Nucleobases and their analogs are fundamental biomolecules that likely served as basic building blocks for the continuous development of life on earth. The formation of these nucleobases from simple prebiotically plausible organic compounds is thus of critical importance to our understanding of the emergence of life. The observation[4−7] that one simple molecule, formamide ($HCONH_2$), is a potential abiotic source of nucleobases and their analogs is profoundly interesting. The synthesis of nucleobases in neat formamide has been explored experimentally.[4,5,8−16] These studies revealed that formamide generates all the essentials (HCN and water) necessary for the synthesis of purine complexes.[4,5,17] Various experimental studies have suggested different abiotic mechanistic pathways for the formation of purines starting from the simple molecules such as formamide or its dehydration products.[11−18] One recently proposed route for the abiotic syntheses of both purine and adenine from formamide indicates that purine and adenine are formed through initial five-membered ring intermediates, 5-aminoimidazole (for purine) and 4-aminoimidazole-5-carboxamidine (AICN, for adenine);[5] this route resembles the biosynthesis of purine nucleobases.[19] Meanwhile other experimental studies suggested mechanistic route evolutions through a pyrimidine intermediate to purine .[15,16]

Complementary to experimental investigations, the step-by-step mechanisms provided by theoretical analysis of the reaction pathways enable the reasonable justification of various potential reaction routes. Theoretical studies, especially reliable quantum chemical computations, are able to provide details about intermediates and transition states along the reaction pathways. Such information allows a deep understanding of the elementary reactions in the feasible routes. Many recent efforts have been devoted to finding a viable, thermodynamically realistic, step-by-step mechanism that can account for the

Received: May 7, 2013
Revised: July 11, 2013
Published: July 15, 2013

Scheme 1. Self-Catalyzed Pathways from Formamide to Purine

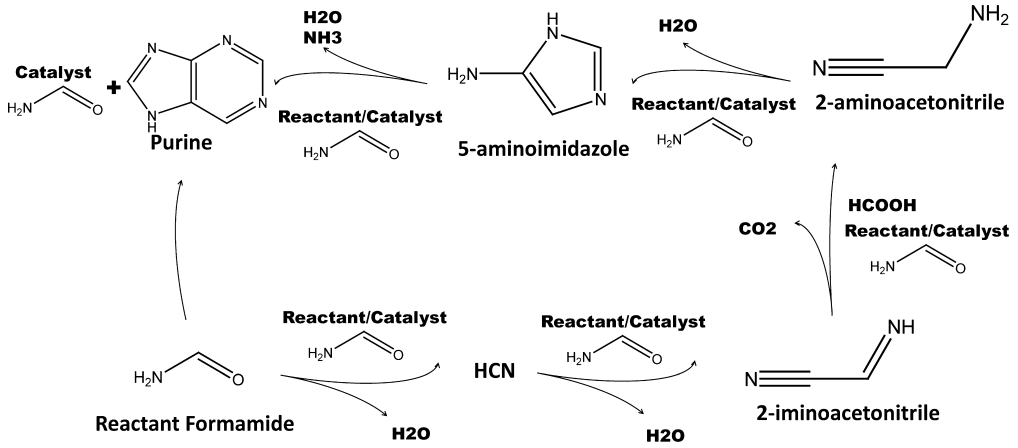

formation of nucleobases. In 2007, Schleyer's group reported the first detailed computational investigation of step-by-step mechanistic pathways from AICN to adenine.[20] Subsequently, in 2012 Sponer et al. reported a density functional theory (DFT) study of the mechanistic pathway of the formation of adenine from formamide through pyrimidine.[21] In these studies, the neutral HCN or the CN^- anion has been adopted as a basic unit for the formation of adenine. Recently, we reported a DFT study of an energetically viable pathway from formamide to purine based on noncatalytic and water-catalyzed approaches.[22] This study provides detailed information of the possible mechanisms similar to those proposed by the Springsteen's group for the biosynthesis of purine nucleobases.[5]

These theoretical studies concluded that the presence of a single or a cluster of water molecules serving as a catalyst is crucial to reduce the rate-controlling reaction energy barriers for acceptable reaction rates.[20−22] Thus, these mechanisms provide reasonable physical pictures for understanding the abiotic syntheses and biosynthesis of nucleobases in mixed formamide/aqueous solutions. However, these water-assisted mechanisms do not account for the reactions that occur in the absence of water, such as those reported by experimental studies, in which case only formamide has been used as reactant.[5,6] It is true that decomposition of formamide may provide water molecules for catalytic procedures. However, previous studies have confirmed that the energy barrier for the dehydration of a formamide molecule is as high as ∼42−44 kcal/mol[22,23] in a noncatalytic processes. Therefore, self-decomposition of formamide under the noncatalytic condition is unlikely to be an energetically viable procedure.

The water molecule acts as both a proton-donor and a proton-acceptor during the formation of nucleobases and purine. Computational investigations of the mechanisms of chemical reactions of neat formamide suggest that a formamide molecule can also serve as both a proton-donor and a proton-acceptor.[23−33] Thus, in the case of the abiotic syntheses of both purine and adenine from anhydrous formamide, it is necessary to study the mechanisms of the formation of nucleobases and purine from formamide in self-catalytic processes. As an expansion of previous studies,[22] we aim to explore the energetically favored pathways of the synthesis of purines based on formamide self-catalyzed mechanisms (Scheme 1). Here we report the step-by-step formamide self-catalytic mechanism of abiotic synthesis of purine from formamide. This represents an effective way to probe energetically viable pathways accounting for the formation of purine nucleobases.

COMPUTATIONAL METHODS

Following the previous study of the mechanistic reaction pathways in the synthesis of purine,[22] the DFT with Becke's three parameter (B3)[34] exchange functional, along with the Lee−Yang−Parr (LYP)[35,36] nonlocal correlation functional (B3LYP), was applied in this investigation. The basis set used was the standard valence triple-ζ basis set, augmented by d-type polarization functions for heavy elements and p-type polarization functions for H, noted as 6-311G(d,p).[37] Our initial study showed that the activation energy barriers predicted at the CCSD(T)/6-311G(d,p), or the MP2/6-311G(d,p), levels of theory for the dehydration steps of formamide in the self-catalyzed pathways are slightly higher than those predicted at the B3LYP/6-311G(d,p) level of theory (see Supporting Information). The studied models have been fully optimized by analytical gradient techniques. In the analysis of harmonic vibrational frequencies, the force constants were determined analytically for all of the complexes either in the local minima or in the transition state structures on the potential energy surface (PES). The stationary structures were confirmed by all positive harmonic frequencies. The corresponding transition state structures (TS) were identified by the existence of single imaginary vibrational frequencies as the saddle points on the corresponding PES. An intrinsic reaction coordinate (IRC) analysis was carried out to confirm that a TS actually connects the corresponding minima. The polarizable continuum model (PCM) self-consistent reaction field of Tomasi and co-workers[38] was employed to evaluate the solvent effects (with a dielectric constant of 108.9 to mimic the solvent formamide) at the same calculation level. The Gaussian-09 package of programs[39] was used for all the computations.

RESULTS

Consistent with our previous study, the discussion below is based on results obtained in gas-phase computations. Inclusion of a PCM model may also be important in some cases. However, as can be seen from the reported studies by Schleyer's group,[20] the effects of solvent are negligible, especially when a large basis is applied. Moreover, our previous and present studies demonstrate that inclusion of a solvent model with the PCM approximation does not significantly alter reaction activation energy barriers. Also, consistent with the

dx.doi.org/10.1021/jp404540x | J. Phys. Chem. B 2013, 117, 9333−9342

previous report the results and the discussions of the energetic properties are based on the zero-point energy (ZPE) corrected relative energies. For clarity, the relative energy differences, free energy differences, and the corresponding PCM corrected energetic properties are provided as Supporting Information.

1. From Formamide to HCN: Dehydration of Formamide. The mechanistic route to the dehydration of formamide in the self-catalytic mechanism is proposed to include three major steps: (1) a proton transfer from N to O to form the imidic acid tautomer of formamide; (2) a proton exchange between one imidic acid and one amide form of formamide, resulting in two imidic acid formamides; and (3) an interaction between two imidic acids yielding formamide, a water molecule, and HCN (Figure 1). These three main steps

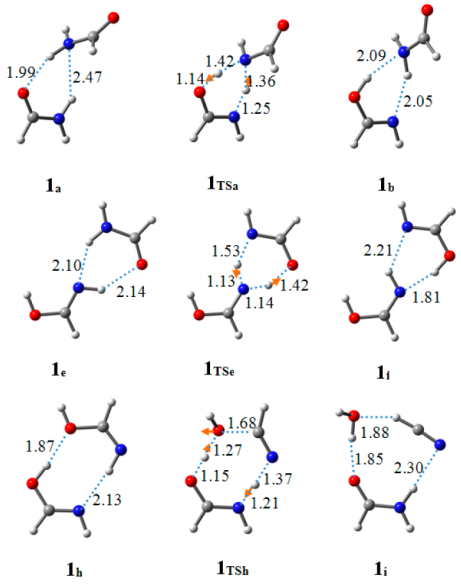

Figure 1. The optimized structures of the complexes in the self-catalyzed dehydration of formamide as the local minima and the transition states on the potential energy surface at B3LYP/6-311G(d,p) level. Atomic distance in angstroms. Orange arrows represent the vibrational mode corresponding to the single imaginary frequency in the transition states. Color representations are the following: red for oxygen, blue for nitrogen, gray for carbon, and white for hydrogen.

are linked through molecular rotation and reorientation steps. The details of the corresponding local mimina and the transition states are listed in the Supporting Information. Apparently, this reaction pathway is much more complicated than the well-known tautomerization-intramolecular proton transfer mechanisms and the water-assisted proton transfer mechanisms. However, the activation energy barriers in the self-catalytic mechanistic route are significantly lower than those in other pathways. In the present DFT calculations, the zero-point energy corrected activation energy barriers corresponding to the three major steps are evaluated to be 26.1, 24.2, and 18.7 kcal/mol, respectively (Figure 2). In comparison, previous studies based on the tautomerization-intramolecular proton transfer mechanism have calculated an activation energy barrier of 44.7 kcal/mol for the tautomerization of formamide to the imidic acid, and 58.3−59.1 kcal/mol (at different levels of theory) for the rate-controlling dehydration of formamide.[22,23] Although the water-assisted mechanism for the dehydration of formamide greatly reduces the activation energy barrier to 33.5

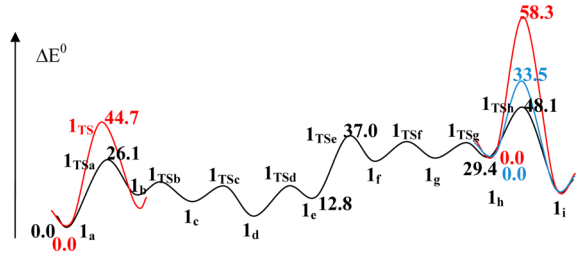

Figure 2. Schematic potential energy profile along the reaction pathway. ΔE^0 is the zero-point energy corrected relative energy (in kcal/mol). Black is for the formamide self-catalyzed reaction. Blue is for the water-catalyzed process. Red is for the noncatalyzed route. It should be noted that the activation energy barrier from **1h** to **1i** is 18.7 kcal/mol in the self-catalyzed process while it is 33.5 kcal/mol in the water-catalyzed process.

kcal/mol,[22,23] it is still more than 7 kcal/mol higher than in the present study. This value is apparently larger than the expected error margin of ±5 kcal/mol of DFT methods on relative energies as compared to high accuracy MO computations. Thus, the self-catalysis mechanism is expected to be more viable, especially in relatively mild reaction conditions.

2. Formation of 2-Iminoacetonitrile: Formiminylation of HCN. Similar to the previous study,[22] two major steps have been identified in the formation of 2-hydroxylaminoacetonitrile and its dehydration. In the first step (formylation), the proton of the HCN transfers to the imidic acid tautomer of formamide resulting in a CN anion. At the same time, one proton migrates from imidic acid to its neighboring formamide, resulting in a protonated formamide (see $\mathbf{2}_b$ in Figure 3). This complex in

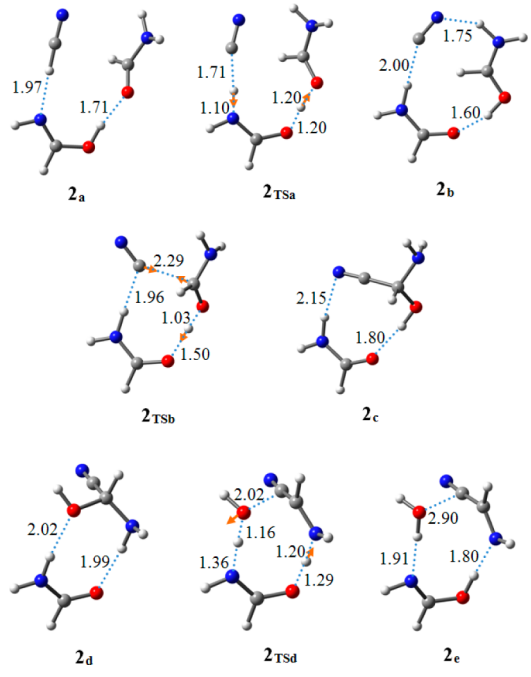

Figure 3. Optimized structures of the complexes in the formamide-catalyzed formiminylation of HCN as the local minima and the transition states on the potential energy surface at the B3LYP/6-311G(d,p) level. Atomic distances are given in angstroms. Orange arrows represent the vibrational mode corresponding to the single imaginary frequency in the transition states. Color representations are the following: red for oxygen, blue for nitrogen, gray for carbon, and white for hydrogen.

dx.doi.org/10.1021/jp404540x | J. Phys. Chem. B 2013, 117, 9333−9342

the near-attacking conformation is a local minimum on the PES. The strongly nucleophilic CN anion in the complex subsequently attacks the carbonyl of the protonated formamide forming a C—C bond to produce the intermediate compound 2-hydroxylaminoacetonitrile ($\mathbf{2}_c$, see Figure 3). The corresponding TS structures ($\mathbf{2}_{TSa}$, and $\mathbf{2}_{TSb}$ in Figure 3) illustrate the formation of the complexes $\mathbf{2}_b$ and $\mathbf{2}_c$. The activation energy barriers of these two transition states are evaluated to be 13.5 and 8.9 kcal/mol, respectively (Figure 4). It should be noted that the reversed reaction from $\mathbf{2}_b$ to $\mathbf{2}_a$ has a very low energy barrier, about 0.5 kcal/mol (1.7 kcal/mol without ZPE correction). Such a low activation energy barrier suggests that the conformer $\mathbf{2}_b$ is a very short-lived clustering structure between the reactant $\mathbf{2}_a$ and the product $\mathbf{2}_c$. Thus the activation energy barrier for the formylation step is based on the transition state $\mathbf{2}_{bTS}$ (evaluated to be 21.9 kcal/mol). Dehydration of 2-hydroxylaminoacetonitrile in the subsequent step is under the influence of formamide. The energy profile of the dehydration step (Figure 4) shows that in the presence of formamide the activation energy barrier for the dehydration of 2-hydroxylaminoacetonitrile is 25.7 kcal/mol, slightly higher than that of the formylation process. It should be noted that the formamide after the dehydration is in the imidic acid form. Therefore, it is the imidic acid form of formamide that acts as a catalyst in the process of the formiminylation of HCN.

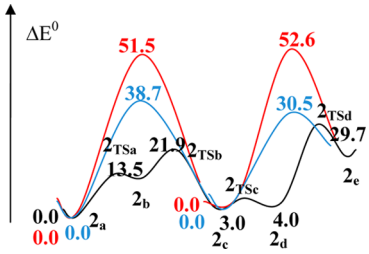

Figure 4. Schematic potential energy profile along the reaction pathway of the formiminylation of HCN. ΔE^0 is the zero-point energy corrected relative energy (in kcal/mol). Black is for the formamide self-catalyzed reaction. Blue is for the water-catalyzed process. Red is for the noncatalyzed route. It is important that the activation energy barrier from 2d to 2e is 25.7 kcal/mol in the self-catalyzed process, which is about 27 kcal/mol lower than in the corresponding noncatalyzed process.

It is interesting that in the presence of two formamide molecules (one in the amide form and the other in the imidic acid form), the dehydration of 2-hydroxylaminoacetonitrile has an activation energy barrier as low as 12 kcal/mol (see energy profile in Figure 5). During the reaction process, the nitrogen atom in the imidic acid tautomer receives one proton from 2-hydroxylaminoacetonitrile. Concurrently, the formamide oxygen donates one proton to the hydroxyl group of 2-hydroxylaminoacetonitrile, leading to the formation of 2-iminoacetonitrile, as shown in Figure 5. Note that the imidic acid tautomer is a final product in the reaction. Thus strictly, this is not a catalytic process.

Previous studies[22] have reported that the uncatalyzed energy barriers of these two steps of the reaction pathway (formylation and dehydration) are 51.5 and 68.2 kcal/mol. However, catalysts greatly increase the reaction rates. In the water-catalyzed process the activation energy barriers are decreased to 38.7 kcal/mol for formylation and 30.5 kcal/mol for dehydration;[22] our present study indicates that the catalytic effects of formamide (in the imidic acid form) are even more profound.

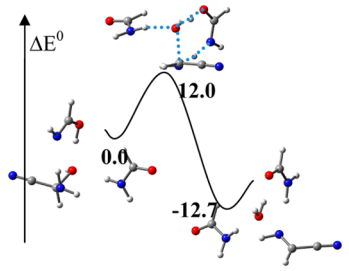

Figure 5. Optimized structures of the complexes and the schematic potential energy profile along the reaction pathway of the dehydration of 2-hydroxylaminoacetonitrile in the presence of two formamide molecules (see text). ΔE^0 is the zero-point energy corrected relative energy (in kcal/mol). Color representations are the following: red for oxygen, blue for nitrogen, gray for carbon, and white for hydrogen.

3. Formation of 2-Aminoacetonitrile: Leuckart Reduction.[40] Formate, a reducing agent, can be generated by the hydrolysis of formamide. The activation energy of direct hydrolysis of formamide was reported to be 38.5 kcal/mol at the same level of theory.[22] Although formate can also be the product of the reaction of two formamides, our study suggested that the corresponding activation energy barrier is around 40 kcal/mol (see Supporting Information). On the other hand, the present study reveals that in the presence of two formamide molecules, the activation energy barrier for the hydrolysis of formamide to generate formate is reduced to 24.9 kcal/mol (Figure 6).

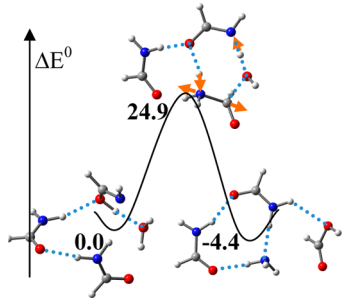

Figure 6. Optimized complex structures and the schematic potential energy profile along the reaction pathway of the hydrolysis of formamide to generate formate in the presence of two formamide molecules (see text). ΔE^0 is the zero-point energy corrected relative energy (in kcal/mol). Color representations are the following: red for oxygen, blue for nitrogen, gray for carbon, and white for hydrogen. Orange arrows represent the vibrational mode corresponding to the single imaginary frequency in the transition state.

The activation energy barrier of the Leuckart reduction of 2-iminoacetonitrile is estimated to be 27.1 kcal/mol in noncatalyzed reactions.[22] Adding two formamide molecules substantially reduces this energy barrier. In the presence of two formamide molecules (one in the amide form and one in the imidic acid form) the reduction of 2-iminoacetonitrile follows three distinct elementary steps (Figure 7), namely: (1) one proton shifts within 2-iminoacetonitrile (from E- to Z-form); (2) one proton transfers from the hydroxyl group of formate to the imino group of 2-iminoacetonitrile through the imidic acid form of formamide, forming the 2-aminoacetonitrile cation; and finally, (3) a hydrogen anion from the deprotonated

dx.doi.org/10.1021/jp404540x | J. Phys. Chem. B 2013, 117, 9333−9342

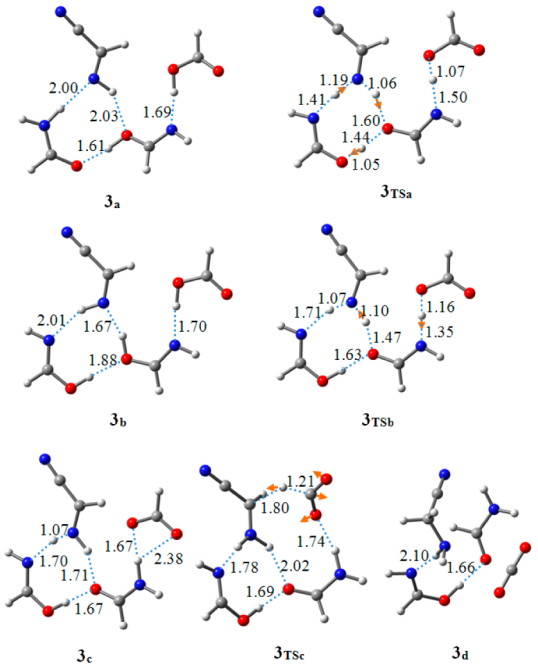

Figure 7. Optimized structures of the complexes in the formamide-catalyzed Leuckart reduction as the local minima and the transition states on the potential energy surface at the B3LYP/6-311G(d,p) level. Atomic distances are given in angstroms. Orange arrows represent the vibrational mode corresponding to the single imaginary frequency in the transition states. Color representations are the following: red for oxygen, blue for nitrogen, gray for carbon, and white for hydrogen.

formate migrates to the C2 position of the 2-aminoacetonitrile cation, yielding 2-aminoacetonitrile and carbon dioxide. The energy profile along the reaction route (Figure 8) reveals that

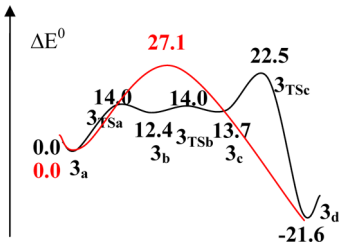

Figure 8. Schematic potential energy profile along the reaction pathway of the Leuckart reduction. ΔE^0 is the zero-point energy corrected relative energy (in kcal/mol). Black is for the formamide self-catalyzed reaction. Red is for the noncatalyzed route.

the activation energy barrier of the first step of the reaction is 14.0 kcal/mol. The activation energy barrier of the following step (step 2) is evaluated to be only 2.0 kcal/mol, and that of the last step is calculated to be 8.8 kcal/mol. The overall energy barrier along this reaction route is approximately to be 22.5 kcal/mol. The Leuckart reduction of 2-iminoacetonitrile is expected to be easy in the formamide solutions. The energy profile of the reaction route also suggests that this reaction is irreversible, the energy barrier for the oxidation of 2-aminoacetonitrile amounts to 44.1 kcal/mol.

4. Formation of 2-Amidinoacetonitrile: Formiminylation of 2-Aminoacetonitrile. Two major steps can be identified in the formiminylation of 2-aminoacetonitrile, that is formylation and dehydration. In the formylation step, the nitrogen of a formamide in the imidic acid form accepts a proton from the amino group of 2-aminoacetonitrile, while the carbonyl carbon of the second formamide attaches to the N atom of the deprotonated amino group of 2-aminoacetonitrile, forming an N—C single bond ($\mathbf{4}_a$, $\mathbf{4}_b$ in Figure 9). The

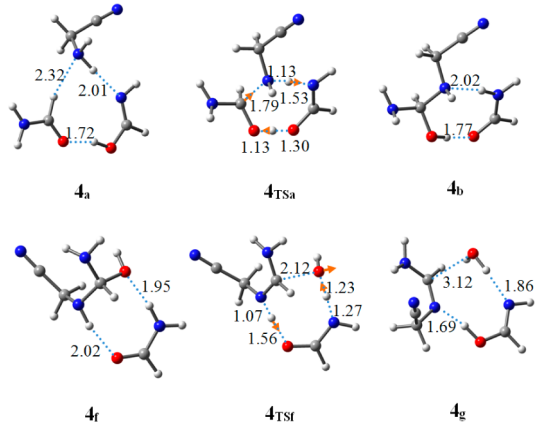

Figure 9. Optimized complex structures in the formamide-catalyzed formiminylation of 2-aminoacetonitrile as the local minima and the transition states on the potential energy surface at the B3LYP/6-311G(d,p) level. Atomic distances are given in angstroms. Orange arrows represent the vibrational mode corresponding to the single imaginary frequency in the transition states. Color representations are the following: red for oxygen, blue for nitrogen, gray for carbon, and white for hydrogen.

structure of the corresponding TS ($\mathbf{4}_{TSa}$) illustrates this process (Figure 9). Four conformational rearrangements, each with low activation energy barriers, follow the formylation and lead to the generation of the near-attacking structure ($\mathbf{4}_f$) of the dehydration step. The subsequent dehydration of $\mathbf{4}_f$ leads to the formation of 2-amidinoacetonitrile. In this step, the hydroxyl group of the intermediate $\mathbf{4}_f$ interacts with the proton of the amino group of the catalytic formamide, forming a water molecule as a leaving group. Meanwhile the proton of the secondary amino group on the 2-position of the formylated 2-aminoacetonitrile migrates to the deprotonating formamide, resulting in 2-amidinoacetonitrile and the formamide imidic acid tautomer. The corresponding TS structure ($\mathbf{4}_{TSf}$) depicted in Figure 9 illustrates this dehydration process. It is important to note that while the untautomerized formamide is a reactant, it is the formamide in the imidic acid form that serves as the catalyst in this formiminylation reaction. The activation energy of the formylation step in this reaction is 21.0 kcal/mol as shown in the energy profile in Figure 10. In comparison, the activation energy barrier of the formylation of 2-aminoacetonitrile reaches 46.1 kcal/mol in the noncatalyzed reaction and 34.3 kcal/mol in the water-catalyzed process. On the other hand, an examination of the energy profile along the reaction pathway indicates that the energy barrier of the dehydration process is 13.4 kcal/mol, much lower than that in the noncatalyzed process (34.0 kcal/mol at the same level of theory). Thus, this reaction is energetically favorable as compared to previously reported investigations.[22]

5. The Formation of 5-Aminoimidazole: Five Membered Ring-Closing. Two main steps are required in the formation of 5-aminoimidazole from 2-amidinoacetonitrile: ring-closing and H-migration. In the presence of the imidic acid tautomer of formamide, ring-closing takes place in a process

dx.doi.org/10.1021/jp404540x | J. Phys. Chem. B 2013, 117, 9333−9342

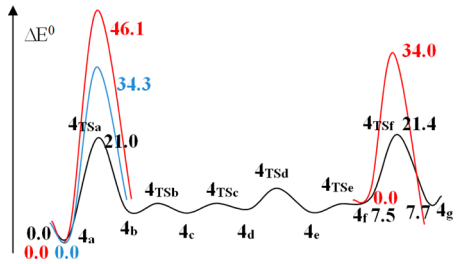

Figure 10. Schematic potential energy profile along the reaction pathway of the formiminylation of 2-aminoacetonitrile. ΔE^0 is the zero-point energy corrected relative energy (in kcal/mol). Black is for the formamide self-catalyzed reaction. Blue is for the water-catalyzed process. Red is for the noncatalyzed route.

accompanied by a proton transfer from $-NH_2$ of 2-amidinoacetonitrile to N of the formamide tautomer. A second concurrent proton transfer from −OH of the same tautomer to −CN of 2-amidinoacetonitrile forms the imidazoline compound (5-iminoimidazoline, Figure 11) as well as a canonical

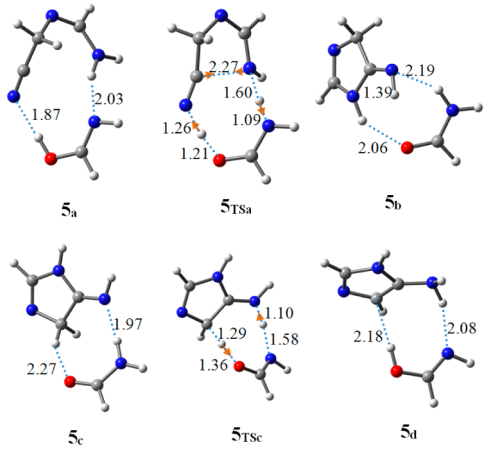

Figure 11. Optimized structures of the complexes in the formamide-catalyzed formation of 5-aminoimidazole from ring-closing as the local minima and the transition states on the potential energy surface at the B3LYP/6-311G(d,p) level. Atomic distances are given in angstroms. Orange arrows represent the vibrational mode corresponding to the single imaginary frequency in the transition states. Color representations are the following: red for oxygen, blue for nitrogen, gray for carbon, and white for hydrogen.

form of formamide. The generated formamide relocates to a position bridging the $-CH_2-$ at the 4-position of the imidazoline ring and the N atom of the imino group on the 5-position. Subsequently, by accepting a proton from the $-CH_2-$ at the 4-position of the imidazoline ring and at the same time by donating a proton to the imino group of the ring compound, this bridging formamide reacts with the 5-iminoimidazoline, yielding 5-aminoimidazole and the imidic acid form of formamide. The energy profile of this reaction route depicted in Figure 12 demonstrates that the activation energy barrier of the ring-closing step is evaluated to be 27.2 kcal/mol and that of the H-migration step is computed to be 20.9 kcal/mol in the presence of formamide (imidic acid form) as a catalyst. In the absence of a water molecule, either ring-closing or intramolecular proton transfer has been reported to have high energy barriers for both processes (57.8 kcal/mol for the former and 68.1 kcal/mol for the latter).[22] Even in the

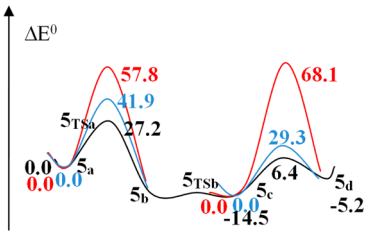

Figure 12. Schematic potential energy profile along the reaction pathway of the formation of 5-aminoimidazole. ΔE^0 is the zero-point energy corrected relative energy (in kcal/mol). Black is for the formamide self-catalyzed reaction. Blue is for the water-catalyzed process. Red is for the noncatalyzed route.

presence of catalytic water the activation energy barrier of the ring-closing is still high as 41.9 kcal/mol.[22] Therefore, the formation of the 5-aminoimidazole through the ring-closing reaction route should follow the imidic acid form of formamide-catalyzed ring-closing and H-migration mechanism.

6. Formation of (Z)-N′-(1H-Imidazol-5-yl)-formamidine: Formiminylation of 5-Aminoimidazole. Similar to the previous formiminylations, the formiminylation of 5-amimoimidazole also consists of two main steps: formylation and dehydration. In the presence of both the imidic acid and amide tautomers of formamide, formylation of 5-aminoimidazole leads to the formation of an intermediate, (S)-(1H-imidazol-5-ylamino)(amino)methanol ($\mathbf{6_b}$ in Figure 13) and an amide form of formamide. In the successive

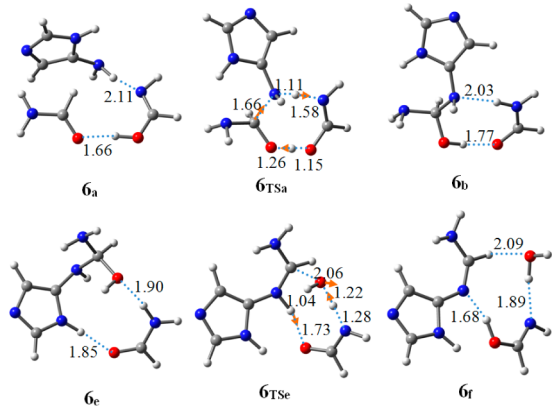

Figure 13. Optimized structures of the complexes in the formamide-catalyzed formiminylation of 5-amimoimidazole as the local minima and the transition states on the potential energy surface at the B3LYP/6-311G(d,p) level. Atomic distances are given in angstroms. Orange arrows represent the vibrational mode corresponding to the single imaginary frequency in the transition states. Color representations are the following: red for oxygen, blue for nitrogen, gray for carbon, and white for hydrogen.

dehydration process, the hydroxyl group attaches to the proton on the N atom of the neighboring formamide molecule, and subsequently leaves as a water molecule. Meanwhile, a proton on the secondary amino group at the 5-position of the imidazole group migrates to the O atom of the same formamide, yielding N′-(1H-imidazol-5-yl)formamidine ($\mathbf{6_f}$ in Figure 13) and an imidic acid tautomer. It should be mentioned that this N′-substituted formamidine species could possess either a Z- or E- configuration. However, only the Z-isomer leads to the formation of purine in the subsequent reactions. The activation energy barrier for the formylation of 5-

dx.doi.org/10.1021/jp404540x | J. Phys. Chem. B 2013, 117, 9333−9342

aminoimidazole is evaluated to be 19.9 kcal/mol (which is 46.1 kcal/mol in the noncatalyzed process and 34.0 kcal/mol in the water-assisted process)[22] and that for the dehydration process is calculated to be 14.0 kcal/mol (34.3 kcal/mol in the noncatalyzed reaction).[22] Figures 13 and 14 display the energy

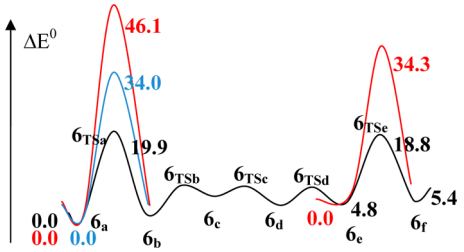

Figure 14. Schematic potential energy profile along the reaction pathway of the formiminylation of 5-aminoimidazole. ΔE^0 is the zero-point energy corrected relative energy (in kcal/mol). Black is for the formamide self-catalyzed reaction. Blue is for the water-catalyzed process. Red is for the noncatalyzed route.

profile and the relevant structures of the intermediates and the transition states formed during the reactions leading to the formation of (Z)-N′-(1H-imidazol-5-yl)formamidine.

7. Formation of (1E)-N′-((Z)-(1H-Imidazol-5-ylimino)-methyl)formamidine: Formiminylation of N′-(1H-Imidazol-5-yl)formamidine. In the presence of two tautomers of formamide (the imidic acidic form and the amide form), formylation of N′-(1H-imidazol-5-yl)formamidine results in a formylated intermediate, (Z)-N-((S)-amino(hydroxy)methyl)-N′-(1H-imidazol-5-yl)formamidine (Figure 15). An inversion of the formamidine nitrogen lone-pair electrons follows the formylation step. This inversion process can be identified from the structures 7_b, 7_{TSb}, and 7_c, shown in Figure 15. After relocation of the catalytic formamide to the site near the hydroxyl and the amino group of the formamidine, the subsequent dehydration (by proton transfer through the formamide) eliminates the hydroxyl group and the proton of the neighboring −NH− group, yielding the dehydrated compound, N′-((Z)-(1H-imidazol-5-ylimino)methyl)-formamidine. The energy profile along the reaction route (Figure 16) reveals that the activation energy barrier of the formylation step amounts to 22.4 kcal/mol, much lower than that predicted in the noncatalytic process (49.4 kcal/mol) and in the water-catalyzed reaction step (37.9 kcal/mol).[22] The activation energy barrier corresponding to the inversion of the configuration of the N atom of the formamidine is estimated to be 18.5 kcal/mol. The activation energy barrier for the formamide-assisted dehydration process is 18.5 kcal/mol, about 21.3 kcal/mol lower than that in the corresponding noncatalytic process (39.8 kcal/mol).[22] Consistent with previous formiminylation reactions, the formamide imidic acid tautomer serves as the catalyst and the formamide in the amide form is a reactant.

8. Formation of Purine: Six-Membered Ring Closing and Deamination. Six-member ring-closure takes place as a C−C single bond is formed between the C atom at 4-position of the imidazole group and the C atom of the formamidine. During the C−C single bond creation process, the hydroxyl group and the imino end of the imidic acid form of formamide "lock" the imino N of the imidazole group and the amine tail of the N′-((Z)-(1H-imidazol-5-ylimino)methyl)formamidine through H-bonding (see 8_a through 8_b in Figure 17). This

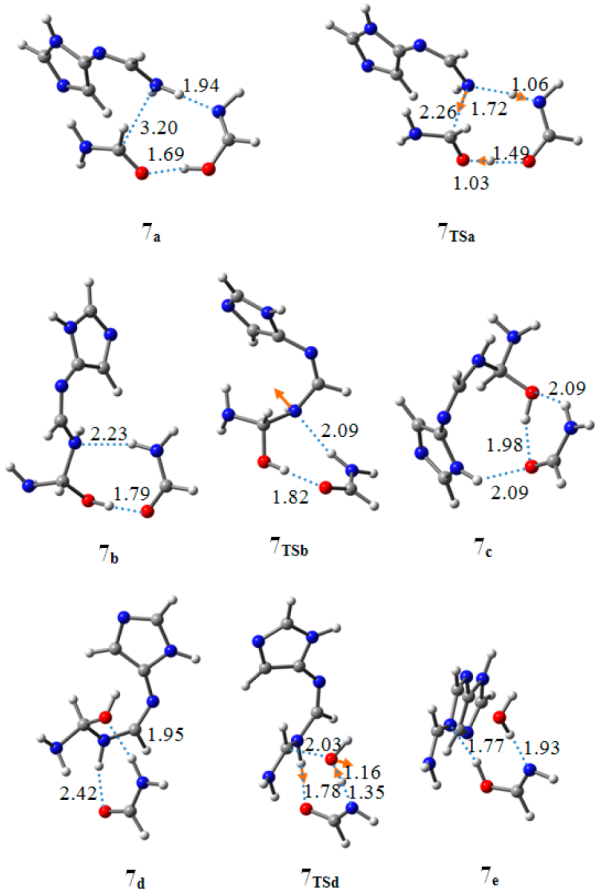

Figure 15. Optimized structures of the complexes in the formamide-catalyzed the formiminylation of N′-(1H-imidazol-5-yl)formamidine as the local minima and the transition states on the potential energy surface at the B3LYP/6-311G(d,p) level. Atomic distances are given in angstroms. Orange arrows represent the vibrational mode corresponding to the single imaginary frequency in the transition states. Color representations are the following: red for oxygen, blue for nitrogen, gray for carbon, and white for hydrogen.

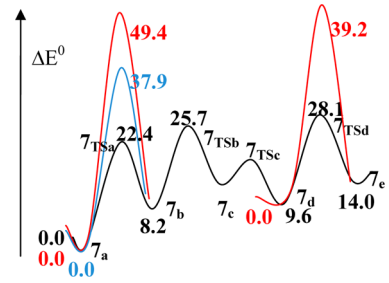

Figure 16. Schematic potential energy profile along the reaction pathway of the formiminylation of N′-(1H-imidazol-5-yl)formamidine. ΔE^0 is the zero-point energy corrected relative energy (in kcal/mol). Black is for the formamide self-catalyzed reaction. Blue is for the water-catalyzed process. Red is for the noncatalyzed route. It is important that the activation energy barrier for 7_d to 7_e is 18.5 kcal/mol in the self-catalyzed process, while it is 39.2 kcal/mol in the noncatalyzed process.

process leads to the formation of (5R,6S)-6,9-dihydro-5H-purine-6-amine (Figure 17).

In the presence of the imidic acid tautomer of formamide, the activation energy barrier of this step is evaluated to be 24.0 kcal/mol (Figure 18). This value is 27.6 kcal/mol when the

dx.doi.org/10.1021/jp404540x | J. Phys. Chem. B 2013, 117, 9333−9342

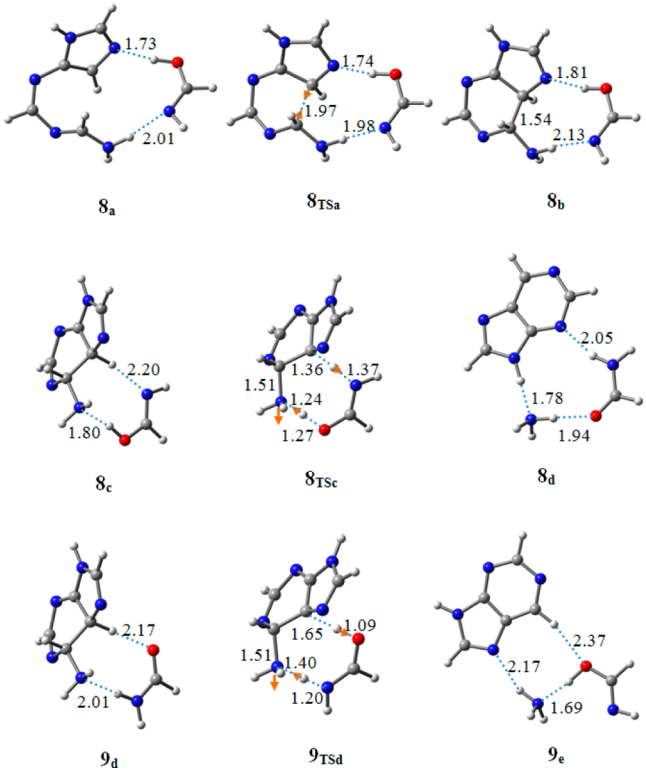

Figure 17. Optimized structures of the complexes in the formamide-catalyzed six-member ring-closing and deamination as the local minima and the transition states on the potential energy surface at the B3LYP/6-311G(d,p) level. Atomic distances are given in angstroms. Orange arrows represent the vibrational mode corresponding to the single imaginary frequency in the transition states. Color representations are the following: red for oxygen, blue for nitrogen, gray for carbon, and white for hydrogen.

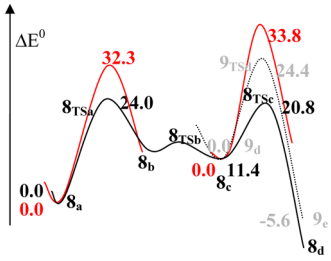

Figure 18. Schematic potential energy profile along the reaction pathway of the six-membered ring-closing and deamination. ΔE^0 is the zero-point energy corrected relative energy (in kcal/mol). Black is for the formamide (imidic acid form) self-catalyzed reaction. Gray (or dashed line) is for the formamide (amide form) self-catalyzed reaction. Red is for the noncatalyzed route.

amide rather than the imidic acid form of formamide acts as catalyst. Compared to the corresponding energy barrier of 32.2 kcal/mol based on the noncatalytic process,[22] six-member ring-closing is energetically favored in formamide solution. The deamination reaction follows as 5H of the dihydro-5H-purin-6-amine migrates to the imino group of the imidic acid tautomer, while the amino group at the 6-position of the purine derivative receives a proton from the hydroxyl group of the formamide, resulting in a purine molecule, an ammonia, and formamide ($\mathbf{8}_c$ to $\mathbf{8}_d$ in Figure 17). Exploration of the detailed potential energy surface reveals that the activation energy of the deamination reaction amounts to 9.4 kcal/mol, compared to 33.8 kcal/mol for the noncatalytic reaction (Figure 18).[22] Deamination can also take place in the presence of the amide form of formamide. In this case, 5H of the dihydro-5H-purin-6-amine transfers to the O atom of formamide, and at the same time one of the protons on the amine group of formamide shifts to the amino group of the purine complex, generating purine, ammonia, and an imidic acid tautomer of formamide ($\mathbf{9}_d$ to $\mathbf{9}_e$ in Figure 17). The corresponding activation energy barrier is 22.4 kcal/mol.

DISCUSSIONS AND CONCLUDING REMARKS

The step-by-step reaction pathway presented herein reveals the details of the formamide self-catalyzed mechanistic route for the synthesis of purine from formamide. All of the reactants and catalysts were found to be generated from formamide through energetically viable reaction routes (with activation energies less than 27 kcal/mol). Formamide in the imidic acid tautomer is found to be the most effective catalyst during the entire reaction pathway. The tautomerization of the normal amide form of formamide to the corresponding imidic acid requires an activation energy of about 26 kcal/mol along the formamide-catalytic reaction pathway. The highest activation energy barrier for the formation of HCN from the imidic acid tautomer is around 25 kcal/mol in the formamide catalyzed process. The hydrolysis of formamide yielding formate proceeds with an activation barrier less than 25 kcal/mol.

Five different types of reactions are presented in this mechanistic route: formylation-dehydration, Leuckart reduction, five-membered ring-closing, six-membered ring-closing, and deamination. Among these reactions, Leuckart reduction and deamination are found to be effectively catalyzed by the presence of two different tautomers of formamide, the imidic acid form and the amide form. In all other reactions (formylation-dehydration and ring-closing), the formamide in imidic acid form is found to be the operational catalyst.

During catalysis of the Leuckart reduction and deamination, one formamide molecule in the imidic acid form tautomerizes into the amide, while another formamide in the amide form tautomerizes to the imidic acid. The activation energies for these catalyzed reactions are less than 23 kcal/mol. Compared to the noncatalytic processes,[22] in which the activation energy barrier for the Leuckart reduction is 27 kcal/mol and that for the deamination is 37 kcal/mol, these steps are expected to follow the formamide-catalyzed route in the formamide solutions under the reported experimental conditions.

In the formiminylation process, catalytic formamide in the imidic acid form tautomerizes to the amide form in the formylation step and subsequently converts back to its original imidic acid form in the subsequent dehydration step. Formylations in the noncatalytic reaction route are found to be energetically demanding steps.[22] The activation energies of the formylations are around 50 kcal/mol. Activation energy barriers corresponding to the dehydration of the formylated products of the intermediates are revealed to be around 40−57 kcal/mol.[22] As presented in this study, these formylation-dehydration steps could be activated by the effects of catalytic formamide during the reaction. With a formamide molecule bridging the proton transfer during the reaction, the activation barriers of formylation steps are found to be less than 21 kcal/mol. One the other hand, the activation energy barrier for the dehydration of the formylated imtermediates ranges from 14 to 26 kcal/mol (dehydration of 2-hydroxylaminoacetonitrile). It is important to note that the activation energy barrier of the dehydration of 2-hydroxylaminoacetonitrile can be further

dx.doi.org/10.1021/jp404540x | J. Phys. Chem. B 2013, 117, 9333−9342

reduced to 12 kcal/mol when an additional formamide molecule is present in the catalytic process. Previous studies revealed that the presence of water reduces the activation energy barrier of the formylation steps to approximately 36 kcal/mol.[22] We conclude that the catalytic effects of water are significantly lower than formamide.

In the five-membered ring-closing and subsequent proton transfer, catalytic formamide in the imidic acid form tautomerizes to the amide form in the ring-closing step and then returns to its original imidic acid form in the subsequent proton transfer step. The corresponding activation energy barriers are reasonable (about 27 kcal/mol for the ring-closing and 21 kcal/mol for the proton transfer) for the reaction to proceed under relatively mild conditions. Without the presence of a catalyst, the five-membered ring-closing and the subsequent intramolecular proton transfer are unlikely to advance due to their high energy barriers (over 60 kcal/mol).[22] Even with water bridges, these two reaction steps are impeded by activation energy barriers up to 42 kcal/mol (ring-closing step) and 29 kcal/mol (proton transfer step).[22]

Overall, the five-membered ring-closing is the rate-determining step in the present mechanistic routes, which is consistent with speculation in the previous mechanism investigation.[22] Also, this finding is consistent with the experimental observations that the longest reaction time is needed for this step in the synthesis.[5] The activation energy of this rate-controlling step (ca. 27 kcal/mol) is significantly lower than the rate-determining step (ca. 34 kcal/mol) in the pathways from AICN described by Schleyer's group[20] and that in the pyrimidine pathway (ca. 44 kcal/mol) reported by Sponer et al.[21] The mechanistic pathway reported herein is energetically favored over the formation of adenine through the pyrimidine route.

The beauty of the formamide self-catalyzed mechanism detailed herein is that this route represents the simplest possible reaction pathway yet proposed. All the reactants and catalysts needed in the reaction are generated from a single compound, formamide, through energetically viable pathways. The activation energy barrier for the rate-controlling step along this route is at least 7 kcal/mol lower than previous theoretical investigations have indicated.[20−22] The information revealed in the present study should benefit further exploration of new and effective synthetic routes for the abiotic formation of nucleic acid bases and other biologically relevant molecules.

■ ASSOCIATED CONTENT

Supporting Information

Energy profile comparison of pathway from formamide to HCN at B3LYP/6-311G(d,p), MP2/6-311G(d,p), and CCSD-(t)/6-311G(d,p) levels, respectively; structures of the intermediates and transition states for the reactions; potential energy profile for interactions of two formamides to produce formate and hydrogen cyanide; potential energy profile of interactions of two formamides to produce formate and hydrogen cyanide catalyzed by one formamide; Table SI listing the enthalpies, free energies, and the SCF energies of all the structures in the studied pathways at B3LYP/6-311G(d,p) level. This material is available free of charge via the Internet at http://pubs.acs.org.

■ AUTHOR INFORMATION

Corresponding Author

*E-mail: (J.G.) jiande@icnanotox.org; (J.L.) jerzy@icnanotox.org.

Notes

The authors declare no competing financial interest.

■ ACKNOWLEDGMENTS

This work was jointly supported by NSF and the NASA Astrobiology Program under the NSF Center for Chemical Evolution, CHE1004570. We would like to thank the Mississippi Center for Supercomputing Research for a generous allotment of computer time. M.T.N. thanks the KU Leuven Research Council (IDO program on exoplanets).

■ REFERENCES

(1) *The RNA World: The Nature of Modern RNA Suggests a Prebiotic RNA World*; Gesteland, R. F., Cech, T., Atkins, J. F., Eds.; Cold Spring Harbor monograph series; Cold Spring Harbor Laboratory Press: Cold Spring Harbor, NY, 2006.

(2) *The Origins of Life on Earth*; Miller, S. L., Orgel, L. E., Eds.; Prentice −Hall: Englewood Cliffs, NJ, 1974.

(3) *Earth's Earliest Biosphere: Its Origin and Evolution*; Schopf, J. W., Ed.; Princeton University Press: Princeton, 1983.

(4) Saladino, R.; Crestini, C.; Ciciriello, F.; Costanzo, G.; Di Mauro, E. Formamide Chemistry and the Origin of Informational Polymers. *Chem. Biodiversity* **2007**, *4*, 694−720.

(5) Hudson, J. S.; Eberle, J. F.; Vachhani, R. H.; Rogers, L. C.; Wade, J. H.; Krishnamurthy, R.; Springsteen, G. A Unified Mechanism for Abiotic Adenine and Purine Synthesis in Formamide. *Angew. Chem., Int. Ed.* **2012**, *51*, 5134−5137.

(6) Yamada, H.; Okamoto, T. A One-step Synthesis of Purine Ring from Formamide. *Chem. Pharm. Bull.* **1972**, *20*, 623−624.

(7) Bredereck, H.; Effenberger, F.; Rainer, G.; Schosser, H. P. Säureamid-Reaktionen XXXI. Eine einfache synthese des Purins. *Justus Liebigs Ann. Chem.* **1962**, *659*, 133−138.

(8) Saladino, R.; Crestini, C.; Costanzo, G.; Negri, R.; Di Mauro, E. A Possible Prebiotic Synthese of Purine, Adenine, Cytosine, and 4(3H)-Pyrimidinone from Formamide: Implications for the Origin of Life. *Bioorg. Med. Chem.* **2001**, *9*, 1249−1253.

(9) Saladino, R.; Ciamecchini, U.; Crestini, C.; Costanzo, G.; Negri, R.; Di Mauro, E. One-Pot TiO_2-Catalyzed Synthesis of Nucleic Bases and Acyclonucleosides from Formamide: Implications for the Origin of Life. *ChemBioChem* **2003**, *4*, 514−521.

(10) Saladino, R.; Neri, V.; Crestini, C.; Costanzo, G.; Graciotti, M.; Di Mauro, E. Synthesis and Degradation of Nucleic Acid Components by Formamide and Iron Sulfur Minerals. *J. Am. Chem. Soc.* **2008**, *130*, 15512−15518.

(11) Saladino, R.; Crestini, C.; Costanzo, G.; Di Mauro, E. Advances in the Prebiotic Synthesis of Nucleic Acids Bases: Implications for the Origin of Life. *Curr. Org. Chem.* **2004**, *8*, 1425−1443.

(12) Barks, H. L.; Buckley, R.; Grieves, G. A.; Di Mauro, E.; Hud, N. V.; Orlando, T. M. Guanine, Adenine, and Hypoxanthine Production in UV-Irradiated Formamide Solutions: Relaxation of the Requirements for Prebiotic Purine Nucleobase Formation. *ChemBioChem* **2010**, *11*, 1240−1243.

(13) Yamada, H.; Hirobe, M.; Higashiyama, K.; Takahashi, H.; Suzuki, K. T. Detection of I3C-′5N Coupled Units in Adenine Derived from Doubly Labeled Hydrogen Cyanide or Formamide. *J. Am. Chem. Soc.* **1978**, *100*, 4617−4618.

(14) Ochiai, M.; Marumoto, R.; Kobayashi, S.; Shimazu, H.; Morita, K. A facile one-step synthesis of adenine. *Tetrahedron* **1968**, *24*, 5731−5737.

(15) Yamada, H.; Hirobe, M.; Higashiyama, K.; Takahashi, H.; Suzuki, K. T. Reaction mechanism for purine ring formation as studied by ^{13}C-^{15}N coupling. *Tetrahedron Lett.* **1978**, *19*, 4039−4042.

(16) Yamada, H.; Hirobe, M.; Okamoto, T. Formamide Reaction. III. Studies on the Reaction Mechanism of Purine Ring Formation and the Reaction of Formamide with Hydrogen Cyanide. *Yakugaku Zasshi* **1980**, *100*, 489−492.
(17) Ferus, M.; Kubelík, P.; Civi, S. Laser Spark Formamide Decomposition Studied by FT-IR Spectroscopy. *J. Phys. Chem. A* **2011**, *115*, 12132−12141.
(18) Shuman, R. F.; Shearin, W. E.; Tull, R. J. Chemistry of HCN. 1. Formation and Reactions of N-(AL minomethylidene)-diaminomaleonitrile,a n HCN Pentamer and Precursor to Adenine. *J. Org. Chem.* **1979**, *44*, 4532−4536.
(19) Katsigiannis, C.; Mar, A.; Oró, J. Prebiotic synthesis of purines from metabolic intermediates. *Origins Life Evol. Biospheres* **1986**, *16*, 297−298.
(20) Roy, D.; Najafian, K.; von R. Schleyer, P. Chemical evolution: The mechanism of the formation of adenine under prebiotic conditions. *Proc. Natl. Acad. Sci. U.S.A.* **2007**, *104*, 17272−17277.
(21) Sponer, J. E.; Mladek, A.; Sponer, J.; Fuentes-Cabrera, M. Formamide-Based Prebiotic Synthesis of Nucleobases: A Kinetically Accessible Reaction Route. *J. Phys. Chem. A* **2012**, *116*, 720−726.
(22) Wang, J.; Gu, J.; Nguyen, M. T.; Springsteen, G.; Leszczynski, J. From Formamide to Purine: An Energetically Viable Mechanistic Reaction Pathway. *J. Phys. Chem. B* **2013**, *117*, 2314−2320.
(23) (a) Nguyen, V. S.; Abbott, H. L.; Dawley, M. M.; Orlando, T. M.; Leszczynski, J.; Nguyen, M. T. Theoretical Study of Formamide Decomposition Pathways. *J. Phys. Chem. A* **2011**, *115*, 841−851. (b) Nguyen, V. S.; Orlando, T. M.; Leszczynski, J.; Nguyen, M. T. Theoretical Study of the Decomposition of Formamide in the Presence of Water Molecules. *J. Phys. Chem. A* **2013**, *117*, 2543−2555.
(24) Maeda, S.; Matsuda, Y.; Mizutani, S.; Fujii, A.; Ohno, K. Long-Range Migration of a Water Molecule To Catalyze a Tautomerization in Photoionization of the Hydrated Formamide Cluster. *J. Phys. Chem. A* **2010**, *114*, 11896−11899.
(25) Wang, B.; Cao, Z. Mechanism of Acid-Catalyzed Hydrolysis of Formamide from Cluster-Continuum Model Calculations: Concerted versus Stepwise Pathway. *J. Phys. Chem. A* **2010**, *114*, 12918−12927.
(26) Chaudhuri, C.; Jiang, J. C.; Wu, C.-C.; Wang, X.; Chang, H.-C. Characterization of Protonated Formamide-Containing Clusters by Infrared Spectroscopy and ab Initio Calculations. II. Hydration of Formamide in the Gas Phase. *J. Phys. Chem. A* **2001**, *105*, 8906−8915.
(27) Reckien, W.; Kirchner, B.; Janetzko, F.; Bredow, T. Theoretical Investigation of Formamide Adsorption on Ag(111) Surfaces. *J. Phys. Chem. C* **2009**, *113*, 10541−10547.
(28) Angelina, E. L.; Peruchena, N. M. Strength and Nature of Hydrogen Bonding Interactions in Mono- and Di-Hydrated Formamide Complexes. *J. Phys. Chem. A* **2011**, *115*, 4701−4710.
(29) Hargis, J. C.; Vohringer-Martinez, E.; Woodcock, H. L.; Toro-Labbe, A.; Schaefer, H. F., III Characterizing the Mechanism of the Double Proton Transfer in the Formamide Dimer. *J. Phys. Chem. A* **2011**, *115*, 2650−2657.
(30) Nagashima, K.; Takatsuka, K. Electron-Wavepacket Reaction Dynamics in Proton Transfer of Formamide. *J. Phys. Chem. A* **2009**, *113*, 15240−15249.
(31) Mardyukov, A.; Sanchez-Garcia, E.; Rodziewicz, P.; Doltsinis, N. L.; Sander, W. Formamide Dimers: A Computational and Matrix Isolation Study. *J. Phys. Chem. A* **2007**, *111*, 10552−10561.
(32) Sanchez-Garcia, E.; Montero, L. A.; Sander, W. Computational Study of Noncovalent Complexes between Formamide and Formic Acid. *J. Phys. Chem. A* **2006**, *110*, 12613−12622.
(33) Frey, J. A.; Leutwyler, S. An ab Initio Benchmark Study of Hydrogen Bonded Formamide Dimers. *J. Phys. Chem. A* **2006**, *110*, 12512−12518.
(34) Becke, A. D. Density-functional thermochemistry. III. The role of exact exchange. *J. Chem. Phys.* **1993**, *98*, 5648−5652.
(35) Lee, C.; Yang, W.; Parr, R. G. Development of the Colle-Salvetti correlation-energy formula into a functional of the electron density. *Phys. Rev. B* **1988**, *37*, 785−789.
(36) Miehlich, B.; Savin, A.; Stoll, H.; Preuss, H. Results obtained with the correlation energy density functionals of becke and Lee, Yang and Parr. *Chem. Phys. Lett.* **1989**, *157*, 200−206.
(37) Hehre, W. J.; Radom, L.; Schleyer, P. R.; Pople, J. A. *Ab Initio Molecular Orbital Theory*; Wiley: New York, 1986.
(38) Cossi, M.; Barone, V.; Cammi, R.; Tomasi, J. Ab initio study of solvated molecules: a new implementation of the polarizable continuum model. *Chem. Phys. Lett.* **1996**, *255*, 327−335.
(39) Frisch, M. J.; Trucks, G. W.; Schlegel, H. B.; Scuseria, G. E.; Robb, M. A.; Cheeseman, J. R.; Scalmani, G.; Barone, V.; Mennucci, B.; Petersson, G. A.; Nakatsuji, H.; Caricato, M.; Li, X.; Hratchian, H. P.; Izmaylov, A. F.; Bloino, J.; Zheng, G.; Sonnenberg, J. L.; Hada, M.; Ehara, M.; Toyota, K.; Fukuda, R.; Hasegawa, J.; Ishida, M.; Nakajima, T.; Honda, Y.; Kitao, O.; Nakai, H.; Vreven, T.; Montgomery, J. A., Jr.; Peralta, P. E.; Ogliaro, F.; Bearpark, M.; Heyd, J. J.; Brothers, E.; Kudin, K. N.; Staroverov, V. N.; Kobayashi, R.; Normand, J.; Raghavachari, K.; Rendell, A.; Burant, J. C.; Iyengar, S. S.; Tomasi, J.; Cossi, M.; Rega, N.; Millam, N. J.; Klene, M.; Knox, J. E.; Cross, J. B.; Bakken, V.; Adamo, C.; Jaramillo, J.; Gomperts, R.; Stratmann, R. E.; Yazyev, O.; Austin, A. J.; Cammi, R.; Pomelli, C.; Ochterski, J. W.; Martin, R. L.; Morokuma, K.; Zakrzewski, V. G.; Voth, G. A.; Salvador, P.; Dannenberg, J. J.; Dapprich, S.; Daniels, A. D.; Farkas, Ö.; Ortiz, J. V.; Cioslowski, J.; Fox, D. J. *Gaussian 09*, revision A.1; Gaussian, Inc.: Wallingford, CT, 2009.
(40) Moore, M. L. *Organic Reactions*; Adams, R., Bachmann, W. E., Blatt, A. H., Fieser, L. F., Johnson, J. R., Eds.; John Wiley and Sons: New York, 1949; Vol. *5*, pp 301−330.